Quasicharacteristic radiation of relativistic electrons at orientation motion in lithium halides crystals along charged planes and axes

N V Maksyuta, V I Vysotskii, S V Efimenko
Taras Shevchenko National University of Kiev, Kiev 01601, Ukraine

E-mail: maksyuta@univ.kiev.ua

Abstract. The paper deals with the investigation of the orientation motion of relativistic electrons in charged (111) planes and charged [110] axes of lithium halides ionic crystals of LiF, LiCl, LiBr and LiI. On the basis of these investigations the spectra of quasicharacteristic radiation for the electron beams with various Lorentz-factors both in planar and axial cases have been calculated numerically.

1. Introduction

The given paper is a continuation of some papers dedicated to the investigation of the processes of the channeling and quasicharacteristic radiation (QCR) of relativistic electrons in charged planes and axes of LiM crystals having NaCl-type structure. Thus, in [1] the interaction potential of relativistic electrons with the charged (111) planes of LiH crystal has been calculated. More detailed research of similar potentials at M = H, D is given in [2] where a comparative analysis of analytically calculated QCR spectra with experimentally measured in [3] has been also done. The paper [4] gives analogous calculations for the case of M = F and the comparison of analytically calculated QCR spectra with experimental data given in [5] for three values of Lorentz-factor have been also made.

The given paper investigates the channeling of relativistic electrons in main charged (111) planes and main charged [110] axes of lithium halides of (M = F, Cl, Br, I). For such regime of motion some corresponding wave functions, energy levels of the channeling motion and QCR spectra were calculated by numerical solutions of Schrödinger equations.

2. The calculation of interaction potentials of electrons with the charged (111) planes of lithium halides crystals

Describing two 1s-electrons by a wave function of the form $\psi_1(r)=\sqrt{\mathrm{Z}^*/\pi a_0}\exp\left(-\mathrm{Z}^* r/a_0\right)$ and one 2s-electron (localized near lithium nucleus with the probability of $1-\alpha$) by a wave function of the form $\psi_2(r)=1/\sqrt{32\pi a_0}\,(2-r/a_0)\exp(-r/2a_0)$, we find the following expression for one-particle potential of Li^+ ion:

$$\varphi_+(r)=e\left\{2\left(\frac{\mathrm{Z}^*}{a_0}+\frac{1}{r}\right)\exp\left(-\frac{2\mathrm{Z}^* r}{a_0}\right)+\frac{(1-\alpha)\,f(r)}{a_0^3}\exp\left(-\frac{r}{a_0}\right)+\frac{\alpha}{r}\right\}. \qquad (1)$$

Here a_0 is the Bohr radius; $\mathrm{Z}^*=\mathrm{Z}_{\mathrm{Li}}-\beta=43/16$ is the screened charge of nucleus of Li^+ ion; $\beta=5/16$ is the screening parameter regarding Li^+ nucleus and calculated by a variation method taking into account the fact that every of 1s-electrons partially screens nucleus of Li^+ ion; α is the degree of ionicity of the link, $f(r)=r^2/8+ra_0/4+3a_0^2/4+a_0^3/r$.

One-particle potentials for negatively charged ions of F^-, Cl^-, Br^- and I^- may be presented by Thomas – Fermi approximation [6]

$$\varphi_-(r)=\frac{e(\mathrm{Z}+\alpha)}{r}\chi\left(\frac{r}{R}\right)-\frac{\alpha e}{r}, \tag{2}$$

where Z is the nucleus charge of M^- ion, $R\approx 0.8853a_0Z^{-1/3}$ is the screening radius of Thomas – Fermi, $\chi(x)=\sum_j \alpha_j \exp(-\beta_j x)$. For used in the given paper Moliere, Barrette and Firsov approximations, the constants α_j and β_j correspondingly equal to: $\alpha_j=\{0.1,0.55,0.35\}$, $\beta_j=\{6,1.2,0.3\}$ [6]; $\alpha_j=\{0.4,0.6\}$, $\beta_j=\{2.984,0.474\}$ [7]; $\alpha_j=4j\sinh^2(1.7\beta)\exp(-3.4\beta j)$, $\beta_j=2\beta j$, $j=1,2,...$ [6]. Evidently the potentials (1), (2) satisfy the following boundary conditions:

$$\varphi_+(r)\underset{r\to 0}{\to}3e/r,\ \varphi_-(r)\underset{r\to 0}{\to}\mathrm{Z}e/r,\ \varphi_\pm(r)\underset{r\to\infty}{\to}\frac{\pm\alpha e}{r}. \tag{3}$$

Note that the first two conditions in (3) follow from the requirement that the potentials should be pure Coulomb near nuclei when their charges are not screened by electrons [8].

The potentials of electro-neutral stems of $V_{0\pm}(x)$ of the charged planes of A^+- (111) and B^-- (111) (in the formula (1) the first and the second components and in formula (2) the first component are used) are calculated in a traditional way [6].

The calculation of the potential created by long-range Coulomb components based on the method given in [9]. The sense of this method is the following. At first the Coulomb potentials of ionic crystals (the last components in (1), (2) formulas) are substituted by the screened Coulomb potentials, namely, $\varphi_\pm(r)=\pm\alpha e/r\lim_{b\to\infty}\exp(-r/b)$. Then after these potentials averaging along the planes, we come to the following expression for the summary potential of the full ensemble of the charged planes of (111) of the ionic A^+B^- crystal:

$$V_\pm(x)=2\pi b\alpha eg\lim_{b\to\infty}\sum_{n=-\infty}^{\infty}\left\{\exp\left(-\frac{|x-nd|}{b}\right)-\exp\left(-\frac{|x-nd-d/2|}{b}\right)\right\}, \tag{4}$$

where $d=a/\sqrt{3}$ is the distance between the same charged crystallographic of (111) planes, $g=4/a^2\sqrt{3}$ is the density of atoms in (111) planes, a is the lattice constant of the crystal. If first in the expression (4) pass to the limit there arises a conditionally convergent series. The methods summations of similar series for the ionic crystals of finite dimensions have been proposed in [10]. This paper deals with another approach which may be more correct from a mathematical point of view. First fulfill a decomposition of the potential (4) by one-dimensional vectors $\vec{g}_n=(2\pi n/d)\vec{e}_x$ of the reciprocal lattice (see, for example, [11]). After this we pass to the limit and come to the next expression for $V_\pm(x)$:

$$V_\pm(x)=\frac{4d\alpha eg}{\pi}\sum_{n=0}^{\infty}\frac{\cos\left[2\pi(2n+1)x/d\right]}{(2n+1)^2}. \tag{5}$$

At last, we confirm that the expression (5) is the expansion into a Fourier series of the following periodic function:

$$V_{\pm}(\xi) = -4V_0 \sum_{n=-\infty}^{\infty} \left[|\xi - n| - \frac{1}{4} \right] \theta \left[\frac{1}{2} - |\xi - n| \right], \tag{6}$$

where $\xi = x/d$ is the relative coordinate, $\theta(x)$ is the Heaviside function, $V_0 = V_{\pm}(n) = \pi d \alpha e g/2$. Further the potential (6) must be averaged over thermal oscillations (with using of thermal oscillations amplitudes of u_+ and u_- correspondingly in the planes of A^+ and B^-). For example, figure 1 (a) presents the graph of interaction potential of $U_{\pm}(\xi) = -e\langle V_{\pm}(\xi)\rangle_{u_+,u_-}$, calculated at T = 300 K for LiF (dash-dot curve). The same figure presents by the solid curve the graph of the interaction potential of $U_{0\pm}(\xi) = -e\langle V_{\pm}(\xi)\rangle_{u_+,u_-}$ with electro-neutral shells of (111) planes of LiF crystal, calculated at the same temperature and with usage of Firsov approximation. The graph of the total interaction potential of $U(\xi) = U_{0\pm}(\xi) + U_{\pm}(\xi)$, presented by the curve 1 in figure 1 (b), confirm that a long-range Coulomb interaction potential of $U_{\pm}(\xi)$ essentially transforms the interaction potential of $U_{0\pm}(\xi)$: in the planes of Li^+- (111) the depths of potential wells increase abruptly but in F^-- (111) planes they, in the contrary, essentially decrease. Evidently, analogous conclusions may be done for other lithium halides crystals. The graph of total interaction potentials of $U(\xi)$ at T = 300 K for LiCl, LiBr and LiI crystals (calculated also by Firsov approximation) are presented by the curves 2, 3 and 4 correspondingly.

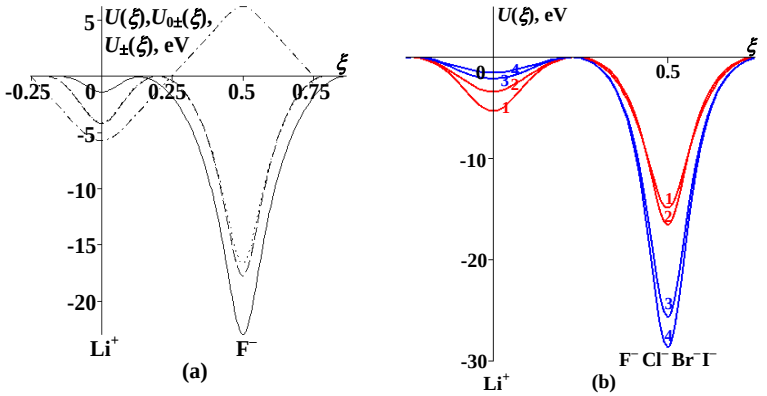

Figure 1. Interaction potentials graphs of electrons channeling along (111) planes: (a) of LiF crystal calculated using Moliere (dot curve) and Barrett (dash curve) approximations; (b) of LiF (curve 1), LiCl (curve 2), LiBr (curve 3) and LiI (curve 4) crystals calculated using Firsov approximation. Figure 1a presents by a solid curve the graph of the interaction potential of electrons with electro-neutral stems of the charged planes in LiF and also dash-dot curve shows a graph of the interaction potential with Coulomb components of the same planes. All the graphs are calculated at T = 300 K.

Note that in the calculation of the considered interaction potentials with B^- planes other approximations may be used. For example, figure 1 (a) presents by a dot curve the potential $U(\xi)$ in the case of LiF crystal calculated by means of Moliere approximation [1] and a dash curve by means of a Barrette approximation correspondingly [7]. However, as further analysis shows, QCR spectra for a LiF crystal coincide with the ones got experimentally (see [5]) only in the case of the channeling of relativistic electrons in potential wells calculated using Firsov approximation. This is just the basis for the choice of this approximation for all other lithium halides crystals.

3. The spectra of quasicharacteristic radiation for the channeling electrons in (111) planes of lithium halides crystals

The method of calculation of QCR was the following. The one-dimensional Schrödinger equation with a relativistic mass (see [6]) reduced to the Sturm – Liouville problem. Then this problem was solved by means of corresponding program from IMSL library of Fortran 90 in the result of which transverse energies of ε_k and their corresponding wave functions $\psi_k(x)$ for all lithium halides crystals at the same Lorentz-factor values which was chosen in [5] for the calculation of QCR spectra in LiF crystal was found. Numerical values of energies ε_k are shown in table 1.

Table 1. Numerical values of transverse energies of ε_k, arising at the channeling of electrons with Lorentz-factors of $\gamma_1 \approx 34$, $\gamma_2 \approx 60.7$ and $\gamma_3 \approx 107.1$ along (111) planes of lithium halides crystals.

ε_k		0	1	2	3	4	5	6	7	8	9
LiF	γ_1	-9.90	-2.98	-2.40	-0.04						
	γ_2	-10.96	-4.49	-3.45	-0.90	-0.53					
	γ_3	-11.83	-6.45	-3.85	-2.70	-1.37	-0.56	-0.02			
LiCl	γ_1	-11.74	-4.13	-2.10	-0.45	-0.07					
	γ_2	-12.79	-6.41	-2.38	-2.22	-0.66	-0.17				
	γ_3	-13.62	-8.44	-4.49	-2.61	-1.78	-1.16	-0.34	-0.15		
LiBr	γ_1	-19.88	-10.37	-3.92	-1.13	-0.55					
	γ_2	-21.15	-13.47	-7.52	-3.30	-1.31	-0.81	-0.20			
	γ_3	-22.13	-16.04	-10.94	-6.80	-3.65	-1.48	-1.46	-0.51	-0.27	-0.01
LiI	γ_1	-22.57	-12.64	-5.57	-1.37	-0.74					
	γ_2	-23.88	-15.94	-9.59	-4.85	-1.72	-0.88	-0.21	-0.02		
	γ_3	-24.89	-18.63	-13.27	-8.81	-5.27	-2.63	-1.00	-0.91	-0.27	-0.06

Figure 2 (a), (b) as illustration presents energy levels and their corresponding wave functions calculated in LiF crystal for the electrons with Lorentz-factor of $\gamma = 60.7$. The arrows in figure 2 (a) present the dipole radiation transitions contribute mainly in QCR spectrum (see figure 3).

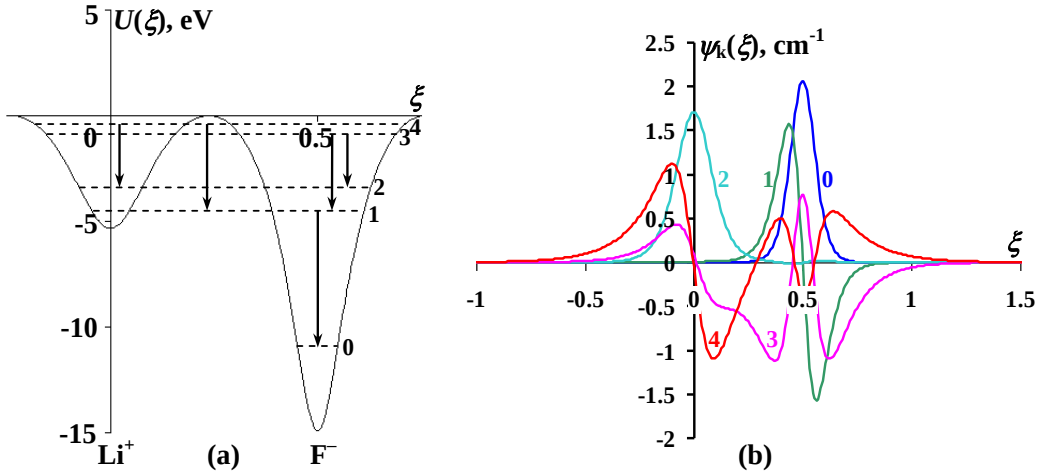

Figure 2. (a) Schematic presentation of energy level systems and radiation dipole transitions arising between them in the case of electrons channeling with a Lorentz-factor of $\gamma = 60.7$ along (111) planes in LiF crystal, (b) system of wave functions corresponding to these energy levels.

From the graphics of wave functions in figure 2 (b) is seen that spontaneous dipole transitions of $1 \to 0$, $3 \to 1$ and $3 \to 2$ are connected with the electrons localized in potential wells of F^-- planes. The transition of $4 \to 2$ is realized on the same electrons which localized mainly in Li^+- planes. At last, the transition of $4 \to 1$ relates to so-called non-direct transitions, since a channeling electron in the result of the loss of the transverse energy changes a region of localization on a spontaneous QCR.

Further, on the basis of the table 1 and using their corresponding wave functions spectral distributions of electron QCR energy were calculated numerically in a dipole approximation on a unit of the path length in correspondence with the following formula:

$$G(\omega) = \frac{1}{\hbar c}\frac{dI}{d\omega} = \frac{e^2 d^2 \omega}{\hbar c^4} \sum_{k=1}^{n-1} \sum_{l=0}^{k-1} \xi_{kl}^2 \Omega_{kl}^2 f\left(\frac{\omega}{2\gamma^2 \Omega_{kl}}\right) \left\langle P_k(\vartheta) \right\rangle, \tag{7}$$

where $f(x) = \left(1 - 2x + 2x^2\right)\theta(1-x)$, $\xi_{kl} = \int_{-\infty}^{\infty} \psi_k(\xi)\xi\psi_l(\xi)d\xi$ is the matrix element of a dipole transition between energy levels of k and l, $\Omega_{kl} = (\varepsilon_k - \varepsilon_l)/\hbar$ is the frequencies of transitions between these levels, $\left\langle P_k(\vartheta) \right\rangle$ is the initial population (averaged by means of a normal distribution function $g(\vartheta) = \left(2\pi\vartheta_0^2\right)^{-1/2} \exp\left(-\vartheta^2/2\vartheta_0^2\right)$, where ϑ_0 is an angular dispersion) of k-th energy level by an electron beam incident on a crystal at an angle of ϑ to some channeling planes. Figure 3 shows the graphs of the dependencies (7) arising in lithium halides crystals at the channeling of electron beams with Lorentz-factors of γ = 34, 60.7, 107.1 ($\vartheta = 0$ mrad, $\vartheta_0 \approx 0.3$ mrad).

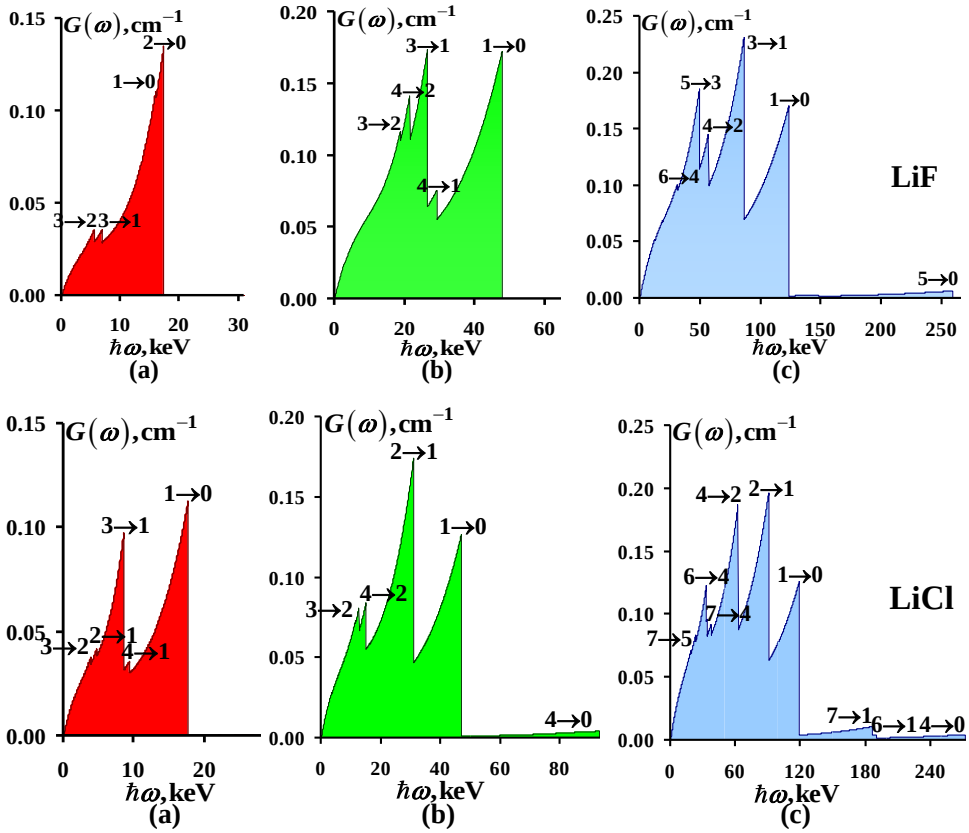

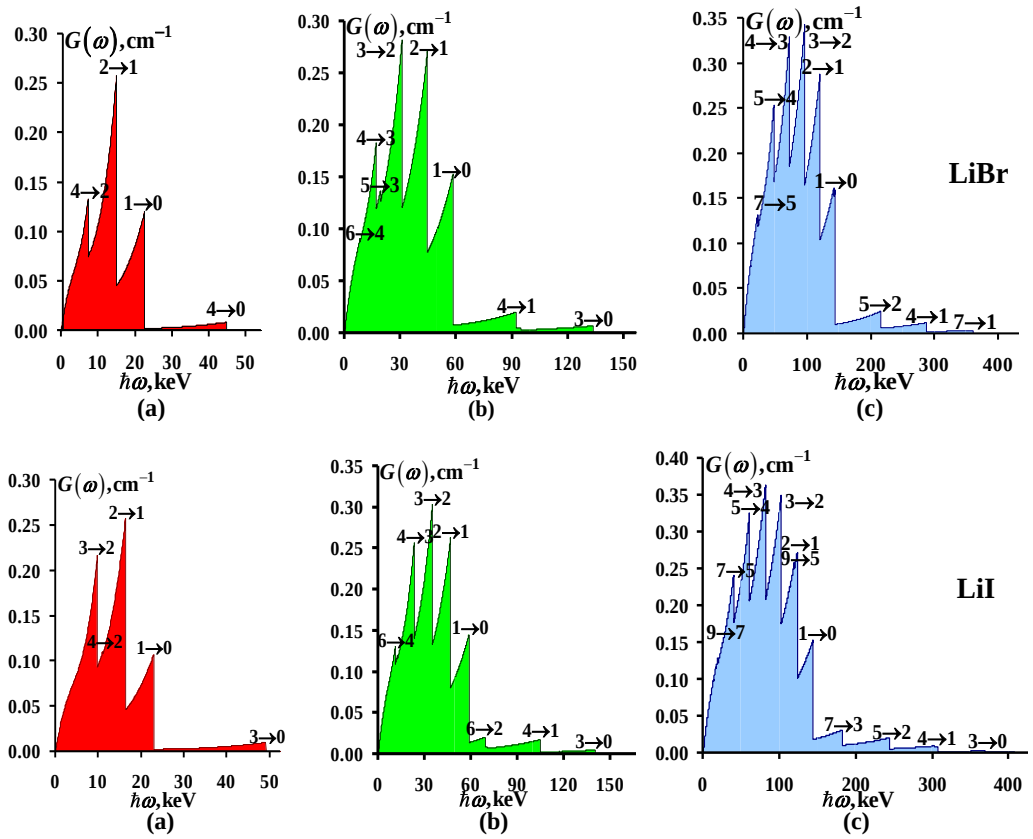

Figure 3. Spectral distributions of QCR energy by an electron per unit path of its motion at a zero angle to (111) planes of LiF, LiCl, LiBr and LiI crystals (the calculations are made for Firsov approximation) accordingly with Lorentz-factors of: (a) $\gamma = 34$, (b) $\gamma = 60.7$ and (c) $\gamma = 107.1$ (an angular dispersion $\vartheta_0 \approx 0.3$mrad). All the graphs present identification between the arising spectral peaks of QCR and displayed dipole radiation transitions.

As it is seen from figure 3 channeling electrons energy increases and also the transition from a crystal LiF to a crystal LiI causes a rise of spectral QCR peaks and their intensities (after a small falling in the case of LiCl crystal) for LiBr and LiI crystals increase approximately in one and a half, two times comparing with the intensities in LiF crystal.

4. The spectra of quasicharacteristic radiation at the channeling of electrons along the charged [110] axes of lithium halides crystals

The interaction potentials (quickly falling with a distance) of $U_{0\pm}(\xi,\eta)$ of relativistic electrons with electro-neutral stems of the charged [110] axes of ionic lithium halides crystals are calculated in a traditional way [6]. The interaction potential of $U_{\pm}(\xi,\eta)$ of the channeling electrons with a Coulomb components of all the ensemble of opposite charged axes is found analogically as in a planar case, namely, it is calculated as the result of the interaction potentials summation (with axes grouping by electro-neutral shells shown in figure 4 (a) (more detailed argumentation for the axial case is shown in [12]). As illustration in figure 4 (b) the 3D-graph is built on one two-dimensional period of $-1/4 \le \xi \le 3/4$, $|\eta| \le 1/4$ in relative coordinates of $\xi = x/a_x$, $\eta = y/a_y$ ($a_x = a/\sqrt{2}$, $a_y = a$) averaged by thermal oscillations of long-range interaction potential of $U_{\pm}(\xi,\eta)$ the electrons with the

system of the charged [110] axes of LiF crystal. Figure 4 (c) presents 3D-graph of the total interaction potential of $U(\xi,\eta)=U_{0\pm}(\xi,\eta)+U_{\pm}(\xi,\eta)$ of the electrons with [110] axes in LiF crystal. It's seen, that in near-barrier regions a potential relief in $\eta=n/2$ planes, where $n=0,\pm1,\ldots$, has minimax points.

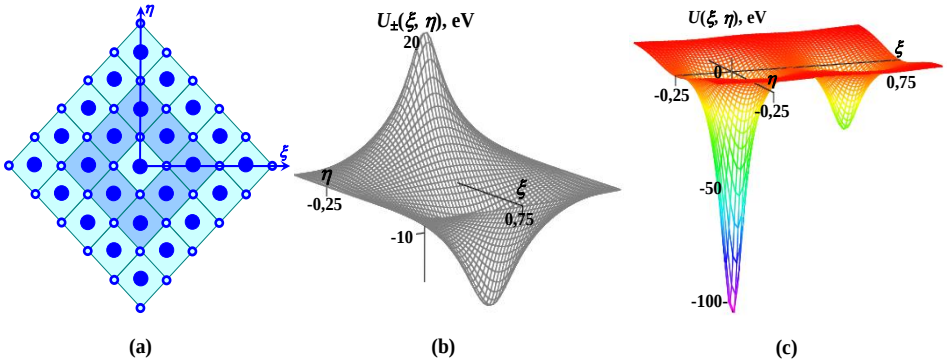

Figure 4. (a) Grouping of the charged axes of A^+B^- ionic crystals of NaCl-type by electro-neutral shells (light circles indicate A^+ axes and dark accordingly B^- axes), (b) 3D-graph of a long-range interaction potential of $U_{\pm}(\xi, \eta)$ of electrons with the system of charged [110] axes of LiF crystal, (c) 3D-graph of total interaction of $U(\xi, \eta)$ of the electrons with [110] axes in LiF crystal. The graphs are calculated at T = 300 K.

In figure 5 (a) in the section of $\eta = 0$ total interaction potentials of electrons with [110] axes for all lithium halides crystals are presented. Note that depths of potential wells in positive and negative charged [110] axes of these crystals correlate in the same way as in the planar case. As the result of numerical solution of the Schrödinger equation (more detailed description see in [12]) for all these potential wells there were found some transverse energy levels and corresponding wave functions for the channeling electrons with a Lorentz-factor of $\gamma = 8$. Analogically planar case on the basis of these data QCR spectra were calculated numerically for dispersion-less electron beams moving regarding [110] axes of lithium halides crystals at zero angles. The graphs of these spectral densities with the indication of dipole radiation transitions are shown in figure 5 (b).

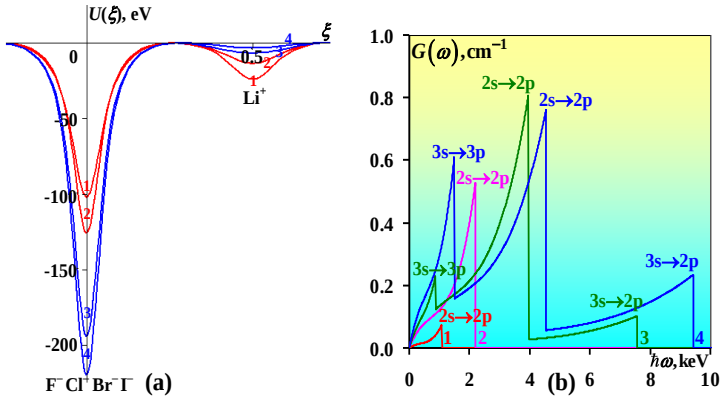

Figure 5. (a) Interaction potentials graphs of electrons channeling along [110] axes in LiF (curve 1), LiCl (curve 2), LiBr (curve 3) and LiI (curve 4) crystals calculated at T = 300 K using Firsov approximation, (b) spectral distributions of QCR energy by the electrons with Lorentz-factors of $\gamma = 8$ per unit path at its flying regarding [110] axes of LiF (curve 1), LiCl (curve 2), LiBr (curve 3), LiI (curve 4) crystals at a zero angle (there is an identification of spectral lines with corresponding radiation transitions).

As it is seen from figure 5 (b), even for a small value of Lorentz-factor the following tendency is evident: at the transition from LiF crystal to LiI one a quantity of radiation transitions increases abruptly and spectral QCR peaks shifting in high-frequency region rise by the intensity. Note that this results correlate with experimental data of orientation motion of electrons with longitudinal energies up to 5 MeV along different axial channels of crystal silicon (see [6, 13]).

5. Conclusions

By using the methods of the calculation of interaction potentials of the charged particles to the charged planes and axes in ionic crystals of NaCl-type there were got analytically interaction potentials of electrons with (111) planes and [110] axes in lithium halides of LiF, LiCl, LiBr and LiI. Wherein the interaction potentials calculation in crystallographic planes built of negative halides ions was made in the framework of Firsov approximation (as it follows from experimental data it is more optimal for LiF crystal).

On the basis of the numerical solutions of Schrödinger equations both in planar and axial cases the systems of energy levels and their corresponding wave functions arising at the channeling of relativistic electrons with various Lorentz-factors were calculated (they coincided with those numerical values which were chosen in [5] and [13]).

Proceeding from these data the QCR spectra in dipole approximation were got numerically both in planar and axial cases. At planar channeling with the transition from LiF crystal to LiI one, QCR energy increases but it is concentrated in the same spectral regions (it is observed for all Lorentz-factors). For an axial case this fact does not take place.

References

[1] Vysotskii V I, Kuz'min R N, Maksyuta N V 1987 *Sov. Phys. JETP* **66** 1150
[2] Maksyuta M V and Vysotskii V I 2012 *Bulletin of the University of Kiev. Series "Radio Physics and Electronics"* **17** 4
[3] Berman B L, Kephart J O, Datz S *et al* 1996 *Nucl. Instr. and Meth. in Phys. Res.* B **119** 71
[4] Maksyuta M V and Vysotskii V I 2012 *Bulletin of the University of Kiev. Series "Radio Physics and Electronics"* **17** 14
[5] Swent R L, Pantell R H, Park H *et al* 1984 *Phys. Rev.* B **29** 52
[6] Bazylev V A and Zhevago N K 1987 *Fast Particles Radiation in a Substance and in External Fields* (Moscow: Nauka)
[7] Barrrett J H 1979 *Phys. Rev.* B **20** 3535
[8] Gombas P 1951 *Statistical theory of an atom* (Moscow: Foreign Literature Publ. House)
[9] Maksyuta N V 2014 *Thesis of the Reports of XLIV Int. Conf. on Physics of Charged Particles Interaction with Crystals*. (Moscow) 19
[10] Korkhmazian N A, Korkhmazian N N, Babadjanyan N E 2003 *J. Tech. Phys.* **73** 1
[11] Ohtsuki Y-H 1983 *Charged Beam Interaction with Solids*, Taylor & Francis Ltd London and New York
[12] Maksyuta N V, Vysotskii V I, Efimenko S V 2015 *Nucl. Instrum. Methods*. B **355** 90
[13] Andersen J U, Bonderup E, Laegsgaard E *et al* 1982 *Nucl. Instrum. Methods*. **194** 209